nature publishing group

Effects of intra-amniotic lipopolysaccharide exposure on the fetal lamb lung as gestation advances

Verena A. Lambermont[1], Elke Kuypers[1], Jennifer J.P. Collins[1], J. Jane Pillow[2], John P. Newnham[2], Graeme R. Polglase[2], Ilias Nitsos[2], Matthew W. Kemp[2], Alan H. Jobe[2,3], Suhas G. Kallapur[2,3] and Boris W. Kramer[1,2]

BACKGROUND: Intra-amniotic lipopolysaccharide (LPS) exposure may affect neonatal outcome by altering fetal lung and immune system development. We hypothesized that intra-amniotic LPS exposure would cause persistent fetal pulmonary responses as the lungs develop *in utero*.

METHODS: Fetal lambs were exposed to intra-amniotic LPS at 118 or at 118 and 123 d of gestational age (GA) with delivery at 125, 133, or 140 d (term = 147 d). Immune responses, PU.1 expression, *Toll-like receptor (TLR)-1,2,4,6* mRNA levels, mast cell levels, and pulmonary elastin deposition were evaluated.

RESULTS: After a single dose of LPS, pulmonary inflammatory responses were observed with increases of (i) PU.1 and *TLR1* at 125 d GA and (ii) monocytes, lymphocytes, *TLR2,* and *TLR6* at 133 d GA. Repetitive LPS exposure resulted in (i) increases of neutrophils, monocytes, PU.1, and *TLR1* at 125 d GA; (ii) increases of neutrophils, PU.1, and *TLR2* at 133 d GA; and (iii) decreases of mast cells, elastin foci, *TLR4,* and *TLR6* at early gestation. At 140 d GA, only PU.1 was increased after repetitive LPS exposure.

CONCLUSION: The preterm fetal lung can respond to a single exposure or repeated exposures from intra-amniotic LPS in multiple ways, but the absence of inflammatory and structural changes in LPS-exposed fetuses delivered near term suggest that the fetus can resolve an inflammatory stimulus *in utero* with time.

Chorioamnionitis, an intrauterine inflammatory response of the chorioamniotic membranes to microorganisms, is a common antenatal exposure for very preterm infants that affects up to 70% of preterm deliveries before 30-wk gestation (1). In chorioamnionitis, the fetus is exposed to inflammation through direct contact with amniotic fluid or via the placental–fetal circulation (2,3). Often, chorioamnionitis is identified only by histological examination of the placental and fetal membranes after birth. Consequently, the duration of fetal exposure to an inflammatory stimulus is seldom known.

Chorioamnionitis affects neonatal outcomes in an organ-dependent way (3), but it is primarily associated with alterations in lung development (4). Chorioamnionitis is associated with a decrease in the incidence of respiratory distress syndrome (5), probably due to induced structural and functional maturity of the lung (6). Conversely, chorioamnionitis is associated with an increase in bronchopulmonary dysplasia (4,7,8) due to inflammatory disruption of lung alveolar and vascular development (9,10). Chorioamnionitis may also negatively affect neonatal outcomes by modulating the fetal immune system (3,11,12). The fetal lung, gut, and skin are directly exposed to the inflammation associated with chorioamnionitis, although other organs and the immune system, which are not in direct contact with the amniotic fluid, can also be affected adversely (3).

Neutrophils, monocytes, and lymphocytes are increased in the alveolar lavages of preterm lambs after a single dose of lipopolysaccharide (LPS) (13). Additionally, intra-amniotic LPS exposure induces (i) maturation of monocytes to alveolar macrophages with increased inflammatory response potentials by inducing hematopoietic transcription factor PU.1 (14) and (ii) cross-tolerance to different Toll-like receptor (TLR) agonists (15). Thus, the naive fetal immune system is capable of complex modulations that can alter subsequent immune function (13). However, our knowledge of the characteristics of these immune responses is limited to short-term exposure to proinflammatory agonists. The persistence of fetal immune modulations following a proinflammatory stimulus and how the duration of exposure to antenatal inflammation may affect the fetal response as gestation advances till near term is poorly understood (13,16). Whether such changes in the immune system persist after a proinflammatory stimulus may enhance understanding of whether preterm/term infants are more susceptible to infections, sepsis, and/or pneumonia later in life (17).

We used an ovine model of chorioamnionitis induced by intra-amniotic LPS to evaluate how exposure interval changed the lung as the fetus matured. Our hypothesis was that intra-amniotic LPS exposures would cause persistent fetal pulmonary responses as the lungs develop *in utero*.

RESULTS

Characterization of Fetuses and Lungs

The body weights and lung weights of LPS-exposed lambs were similar to those of the control group at each gestational

[1]Department of Pediatrics, Maastricht University Medical Center, Maastricht, The Netherlands; [2]School of Women's and Infants' Health, University of Western Australia, Perth, Australia; [3]Department of Pulmonary Biology, Cincinnati Children's Hospital Medical Center, University of Cincinnati, Cincinnati, Ohio. Correspondence: Boris W. Kramer (b.kramer@mumc.nl)

Received 18 April 2013; accepted 27 September 2013; advance online publication 5 February 2014. doi:10.1038/pr.2014.3

age (GA; Table 1), indicating similar growth. The cord blood pH and pCO_2 were not different between groups.

As anticipated, the LPS-exposed lambs delivered at 125 d GA had higher lung gas volumes compared with the control group (Table 1). Increased lung volume after LPS exposure persisted with delivery at 133 d GA. At 140 d GA, the control and the treatment groups had comparable pressure–volume deflation curves. The number of LPS injections did not influence lung gas volumes at any GA.

Pulmonary Inflammation

The total number of leukocytes increased after exposure to LPS at 125 and 133 d GA. Neutrophils, in particular, increased significantly in the bronchoalveolar lavage fluid (BALF) after two injections of LPS (Figure 1a). Monocytes also increased at both 125 and 133 d GA (Figure 1b). Lymphocytes increased only at 133 d GA after a single LPS exposure (Figure 1c). No difference in the total number of neutrophils, monocytes, and lymphocytes after LPS exposure was detected at 140 d GA (Figure 1a–c).

PU.1-Expressing Cells in Lung Tissue

Cells expressing PU.1 increased in the lung tissue after two LPS injections at each gestation (Figure 2a). Compared with PU.1 expression in control lambs (Figure 2b), the expression of PU.1 was high in both alveolar and interstitial cells (Figure 2c). In contrast, a single LPS exposure resulted in only a transiently increased PU.1 expression: increased PU.1 level was evident at 125 d GA, but PU.1 expression was lost at 133 and 140 d GA (Figure 2a).

TLR mRNA in Lung Tissue

TLR1 mRNA levels increased after one and two doses of LPS at 125 d GA (Figure 3a). mRNA levels of *TLR4* and *TLR6* decreased after the two exposures to LPS and subsequent delivery at 125 d GA (Figure 3c–d). However, increased mRNA levels of *TLR2* and *TLR6* were detected at 133 d GA (Figure 3b–d). No significant differences in *TLR* mRNA levels were detected at 140 d GA.

Mast Cells and Clara Cells in Lung Tissue

Mast cells were present in the bronchial wall but not in other regions of lung tissue (Figure 4b,c). At 125 d GA, there was a trend for a decreased number of mast cells with LPS (Figure 4a). The decrease in mast cells was significant after two doses of LPS at 133 d GA. The number of mast cells increased as GA advanced (Figure 4a). A representative Clara cell staining (Figure 4d,e) was performed to demonstrate the specificity of the mast cell staining.

Elastin Expression in the Lung

The elastin foci on alveolar septa were counted on sections from the right upper lobe (Figure 5a). Elastin foci were reduced in number after two LPS injections at 125 d GA. The elastin was localized more diffusely in LPS-exposed lungs (Figure 5c), compared with control lungs, at 125 d GA (Figure 5b). Elastin foci were not different in number or localization in lungs of LPS-exposed and control groups at 133 and 140 d GA.

DISCUSSION

To better characterize the effects of LPS on the fetal lung, we measured a number of variables that could contribute to longer-term adverse effects of fetal exposure to LPS. We used the single exposure at 118 d and the two exposures at 118 and 123 d to parallel our previous reports that demonstrated fetal immune tolerance to LPS (13,16,18). The deliveries at 2, 10, and 17 d after the second exposure allowed evaluation of the persistence of responses during late fetal development.

LPS in the amniotic fluid has a half-life of 1.7 d, with inflammation markers remaining measurable for at least 15 d after administration (19). In this study, intra-amniotic LPS exposure resulted in changes in the fetal lung inflammatory

Table 1. Description of animals

Treatment	No. of animals	BW (kg)	Lung weight (g/kg BW)	Cord blood pH	Cord blood pCO_2	V40 ml/kg BW
Delivered at 125 d GA						
Control	7	3.0 ± 0.1	35.0 ± 0.9	7.28 ± 0.03	65 ± 3	12.1 ± 1.7
2 d LPS	7	3.0 ± 0.1	31.9 ± 1.3	7.31 ± 0.02	62 ± 3	30.0 ± 2.3*
2 + 7 d LPS	7	2.9 ± 0.1	38.5 ± 2.8	7.26 ± 0.03	67 ± 2	33.7 ± 2.5*
Delivered at 133 d GA						
Control	7	4.0 ± 0.3	31.4 ± 1.0	7.20 ± 0.02	74 ± 4	27.8 ± 4.8
2 d LPS	7	4.1 ± 0.1	34.3 ± 1.0	7.20 ± 0.01	74 ± 3	37.9 ± 1.8*
2 + 7 d LPS	5	3.7 ± 0.1	32.0 ± 1.6	7.26 ± 0.02	68 ± 3	38.6 ± 1.1*
Delivered at 140 d GA						
Control	7	5.0 ± 0.2	29.1 ± 0.9	7.25 ± 0.03	67 ± 4	40.9 ± 3.8
2 d LPS	6	5.3 ± 0.1	35.2 ± 3.8	7.18 ± 0.04	80 ± 5	36.1 ± 3.4
2 + 7 d LPS	7	5.0 ± 0.2	33.4 ± 1.8	7.24 ± 0.04	77 ± 6	37.7 ± 3.4

BW, body weight. V40 ml/kg BW, lung volume at 40 cmH_2O per kilogram body weight.
*$P < 0.05$ vs. control group of the same gestational age.

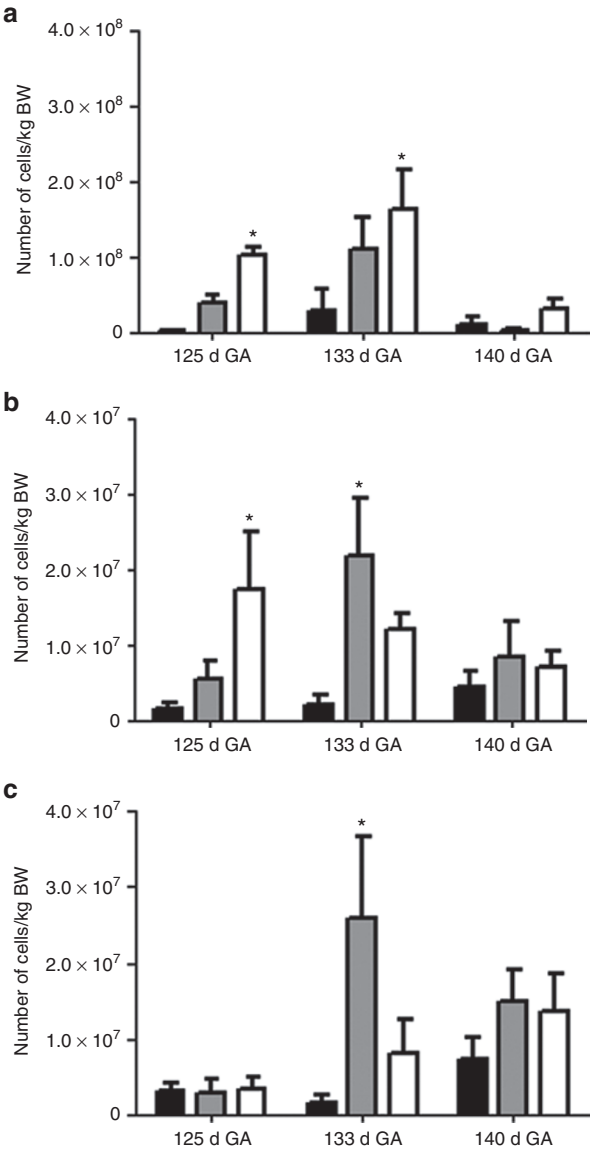

Figure 1. Pulmonary inflammation. Leukocytes were increased in BALF after LPS exposure at gestational ages of 125 and 133 d, with a significant increase of (**a**) neutrophils and (**b**) monocytes at 125 and 133 d GA. (**c**) Lymphocytes were increased after a single dose of LPS at 133 d GA. (**b** and **c**) The *y*-axis was adjusted for the low number of monocytes and lymphocytes. Black bars = sal/sal; grey bars = sal/LPS; white bars = LPS/LPS. **P* < 0.05 vs. control group of the same gestational age. BALF, bronchoalveolar lavage fluid; GA, gestational age; LPS, lipopolysaccharide; sal, saline.

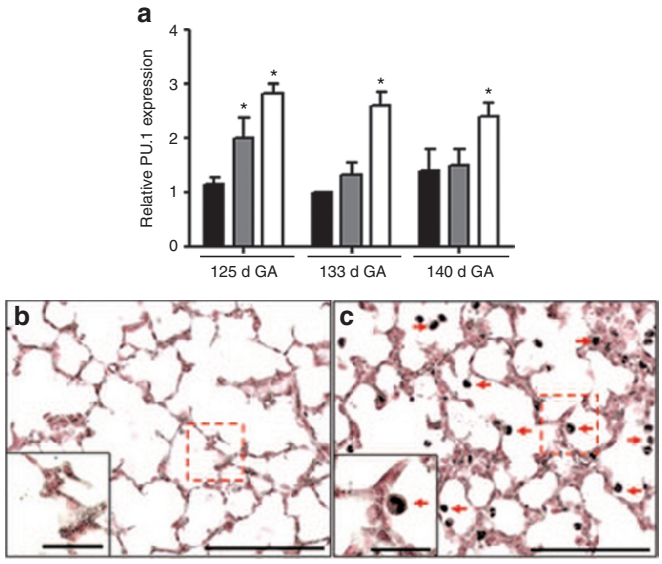

Figure 2. PU.1 expression in lung tissue. (**a**) The PU.1-positive cells in lung tissue exposed to LPS differed significantly from controls at each gestation. Representative staining (original magnification ×200, bar = 100 µm) is shown (**b**) for 125 d GA control animals and (**c**) after two doses of LPS. The high-magnification (original magnification ×400, bar = 25 µm) insets illustrate the strong positivity of cells for PU.1 after exposure to LPS compared with that of controls. Red arrows indicate cells expressing PU.1. Black bars = sal/sal; grey bars = sal/LPS; white bars = LPS/LPS. **P* < 0.05 vs. control group of the same gestational age. GA, gestational age; LPS, lipopolysaccharide; sal, saline.

responses. This is consistent with our previous findings at 125 d GA regarding treatment after one or two doses of LPS (4,20,21). Our findings show that the increase in neutrophils at 133 d was evidence of a persistent response to the initial inflammatory stimulus. Furthermore, two doses of LPS were required to induce significant differences in BALF neutrophil content at 125 d GA. This finding suggests that the pulmonary immune response may be dependent on the intensity and/or persistence of the LPS exposure. The local immune system of the lung seems to remain active until 133 d GA, with increased number of monocytes and lymphocytes. Interestingly, a macrophage response was involved in the pulmonary inflammatory response to LPS in the course of gestation, shown by an increased PU.1 expression. Normally, the fetal lung contains few macrophages, and monocytes mature to macrophages with PU.1 expression after term birth (14,22,23). The lungs of fetal sheep exposed to intra-amniotic LPS expressed PU.1 within 1–2 d, and vacuolated alveolar macrophages could be recovered by lavage several days later (14). We reported that PU.1 expression increased 7 d after a single exposure to LPS but that expression was lost 15 and 22 d later. In contrast, the second exposure 5 d following the first exposure resulted in high PU.1 expression, which persisted until 140 d GA. These observations demonstrate that monocyte to macrophage maturation in the fetal lung can be transient or persistent depending on the characteristics of the inflammatory exposure. *In vitro*, fetal alveolar macrophages responded to TLR agonists similarly to alveolar macrophages from the adult lung (15). The persistence of macrophages could promote inflammation in the fetal lung or in the lung following delivery after TLR stimulation and may lead to an increased susceptibility for neonatal sepsis and pneumonia (17).

TLR mRNA levels were low in the fetal sheep lung relative to the adult lung, and changes in expression are minimal during late gestation (24). Our results demonstrated that changes in *TLR* mRNA levels with LPS exposure differed by TLR, exposure, and interval from exposure. *TLR4* mRNA levels decreased 2 d, but not 7 d, following intra-amniotic injection of LPS. The delayed increases in *TLR 2* and *6* mRNA levels 15 d after the initial exposure to the TLR4 agonist LPS might have clinical implications for the chronic infection and often

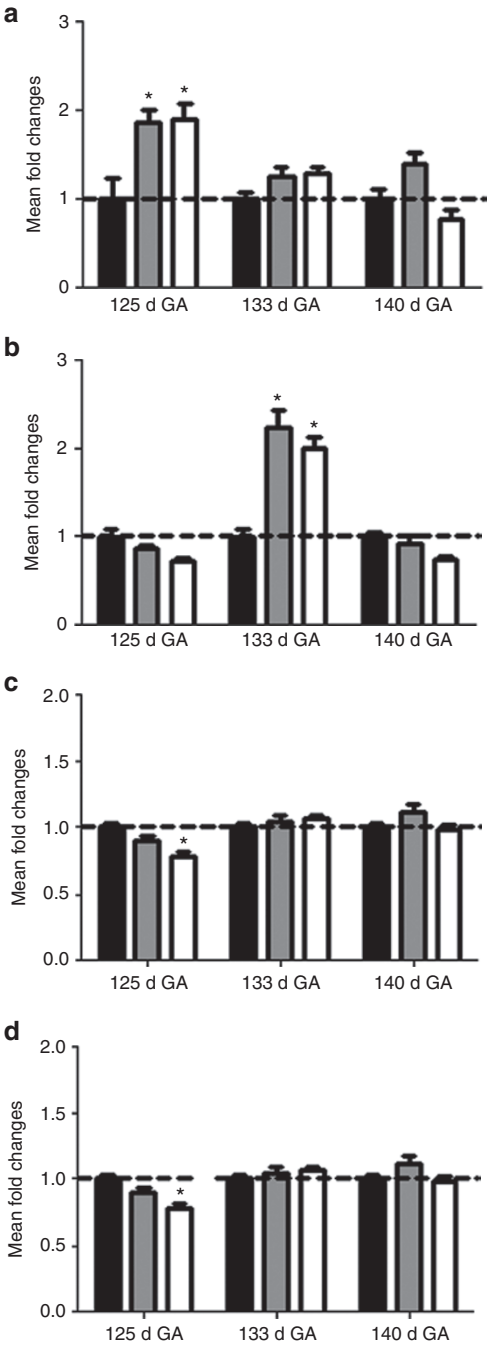

Figure 3. mRNA levels of *TLR 1, 2, 4,* and *6*. (**a**) *TLR1* mRNA level was increased after a single dose and after double doses of LPS at 125 d GA. At 125 d GA, mRNA levels of (**c**) *TLR 4* and (**d**) *TLR 6* were decreased after a double dose of LPS. At 133 d GA, increased mRNA levels of (**b**) *TLR 2* and (**d**) *TLR 6* were detected. No differences in mRNA levels were detected at 140 d GA. Black bars = sal/sal; grey bars = sal/LPS; white bars = LPS/LPS. **P* < 0.05 vs. control group of the same gestational age. GA, gestational age; LPS, lipopolysaccharide; sal, saline; TLR, Toll-like receptor.

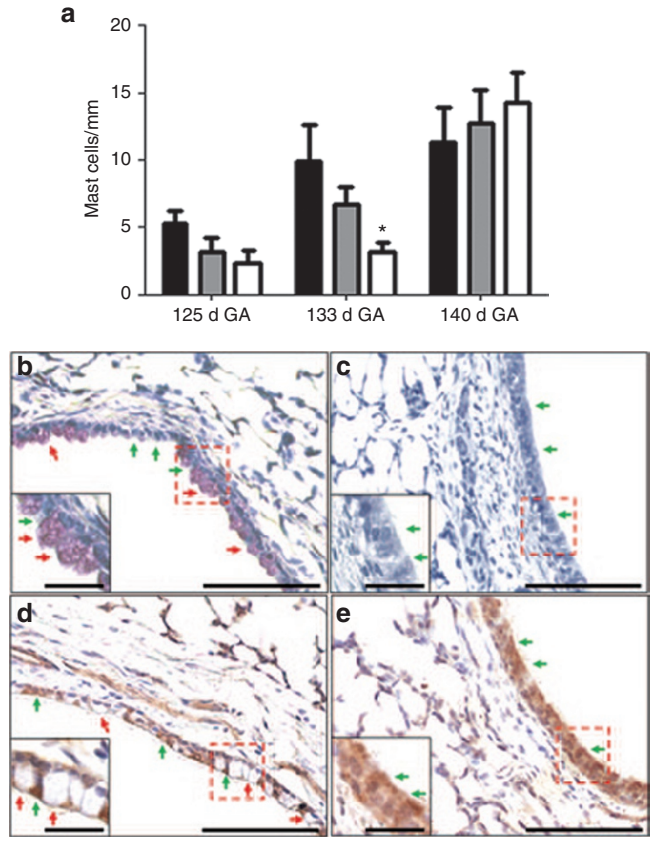

Figure 4. Representative staining and number of mast cells counted in the bronchial wall. There were no changes in the number of mast cells (**a**) as a result of exposure to LPS with one or two doses compared with the control group at 125 and 140 d GA. At 133 d GA, the number of mast cells decreased after repetitive LPS administration. Representative staining (original magnification ×200, bar = 100 μm) is shown in panel (**b**) for 133-d-GA control animals and in panel (**c**), after two doses of LPS. The high-magnification insets (original magnification ×400, bar = 25 μm) illustrate the loss of mast cells after exposure to LPS compared with the number in controls. Panels (**d**) and (**e**) represent the staining for Clara cells in the bronchial wall. Red arrows indicate mast cells, and green arrows indicate Clara cells. Black bars = sal/sal; grey bars = sal/LPS; white bars = LPS/LPS. **P* < 0.05 vs. control group of the same gestational age. GA, gestational age; LPS, lipopolysaccharide; sal, saline.

polymicrobial organisms associated with chorioamnionitis (17). Interestingly, increased *TLR2* and *6* mRNA levels seem to be related to increased monocyte numbers in BALF 15 d after a single injection, indicating an early development of the monocytes (25). It is not clear why there was a resolution of TLR2 and TLR6 to term gestation.

The homeostasis of the airway is also maintained by mast cells. Mast cells in the lower airways contribute to the development of asthma and allergic diseases (26). Mast cells are of interest because of a possible relation between chorioamnionitis, preterm birth, and the development of asthma later in life (27,28). Mast cell activation results in degranulation, leading to the rapid release of inflammatory mediators, such as histamine, proteoglycans, and cytokines, which stimulate the recruitment of other inflammatory cells (29). Mast cells are mostly present near epithelial surfaces such as mucosa of the lungs and the digestive tract (29). In this study, mast cells were found in the bronchial walls of preterm fetal lamb lungs. Although exposure to LPS resulted in a decrease of mast cells in the more immature lambs, mast cell numbers had returned to normal for lambs delivered near term. Our finding of reduced mast cell populations soon after LPS exposure contrasts with our hypothesis that LPS exposure would increase

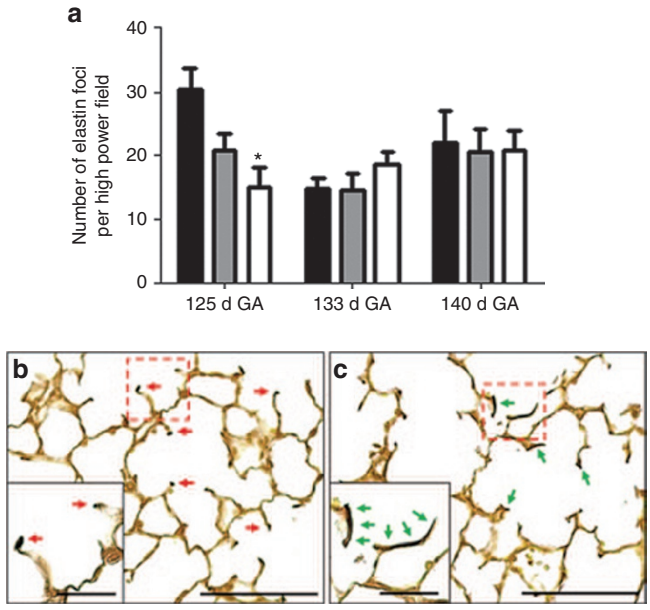

Figure 5. Expression of elastin foci on alveolar septa in lung tissue. Decreased numbers of (**a**) elastin foci were recorded at 125 d GA after a double dose of LPS. At 133 and 140 d GA, the lungs showed no differences after LPS exposure compared with control animal lungs. The high-magnification insets (original magnification ×400, bar = 25 µm) show that the focal depositions of elastin on the tips of alveolar septa, which are strongly present in (**b**) the lungs of controls at 125 d GA, are diminished and diffusely expressed in (**c**) lungs after a double dose of LPS at 125 d GA. (**b** and **c**) High-magnification images (original magnification ×200, bar = 100 µm). Red arrows indicate location of focal expression of elastin, and green arrows indicate diffusely expressed elastin. Black bars = sal/sal; grey bars = sal/LPS; white bars = LPS/LPS. *$P < 0.05$ vs. control group of the same gestational age. GA, gestational age; LPS, lipopolysaccharide; sal, saline.

mast cells. However, repeated fetal exposures to LPS decreased airway responses to methacholine challenge in 7-wk-old lambs (12). The relationship between prenatal inflammation and the mast cell response in the fetal airways has not been studied. Increased levels of mast cells were associated with the development of BPD in one autopsy study (30). Mast cell regulation is complex, depending on the timing of the fetal and postnatal stimuli. Our results demonstrated that fetal exposure to LPS could change mast cell numbers in the fetal lungs. However, the long-term effect of intrauterine exposure to inflammation on mast cell presence and function in postnatal life needs to be determined.

To examine lung structure, elastin foci on alveolar septa were counted on lung sections. Although a double LPS exposure resulted in more diffusely localized elastin foci in the more immature fetal lambs, a more normal distribution with localization of elastin foci at the tips of alveolar septa was reestablished near term, indicating recovery with advancing gestation. Whereas a single LPS exposure can induce structural maturation (4,31), a second LPS exposure may increase the abnormal elastin distribution and alveolar development. In addition, it was demonstrated that prenatal LPS exposure upregulated tropoelastin (soluble precursor of elastin) mRNA levels in lung tissue at the time of secondary septa development, resulting in a more diffuse elastin expression along the alveolar cell wall (32). This might contribute to the abnormal lung structure. The mechanism by which the fetal lung repairs the abnormal elastin response is unknown. Some of the variables in the "recovery" response, detected in part in this study, may be GA at assessment, GA at time of initial exposure (33), and magnitude of the inflammatory responses and/or antenatal steroids (34).

A limitation of our study was that no additional exposure to LPS was given immediately before delivery at the different GAs to challenge the fetal immune system. In human pregnancies affected by chorioamnionitis, fetuses are exposed to bacteria until delivery, which challenges the immune system continuously. In our model, the fetus had a single or a second dose of LPS within a confined GA range, and the proinflammatory stimuli might be less than those occurring in human infants. In this study, we focused on the lungs. From literature, it is known that chorioamnionitis is a multiorgan disease that affects the central nervous system, skin, and the gut in clinics and experimental models (3,35,36). The interaction of the different organs is not very well understood, but the role of the immune system of the fetus, as well as the role of endotoxins in human chorioamnionitis, warrants further research.

In summary, the fetal lung responded to intra-amniotic LPS with changes that might have long-term effects on lung and immune function. Although the abnormalities in elastin distribution did not persist, monocyte to macrophage maturation, selective TLR expression, and mast cell numbers could change at later times after the LPS exposure. How preterm delivery might interact with these changes remains to be determined.

METHODS

Antenatal Treatment

All animal procedures were approved by the Animal Ethics Committee of the University of Western Australia. Pregnant Merino ewes received an intra-amniotic injection with saline (sal, 2 ml; controls) or 10 mg LPS–(*Escherichia coli* 055:B5; Sigma–Aldrich, St. Louis, MO) at 118 and 123 d GA (**Figure 6**). The fetuses were delivered operatively at 125 d ($n = 21$), 133 d ($n = 19$), or 140 d ($n = 20$) gestation (term = 150 d). Each lamb was killed at delivery with an intravenous injection of pentobarbital (100 mg/kg, Valabarb; Jurox, Rutherford, NSW, Australia).

Processing of the Fetal Lung

Lung compliance was assessed by measuring lung gas volumes from pressure–volume curves as a measure of lung maturation. The thorax was opened with a midline incision, and a tracheal tube was inserted and connected to a manometer (37). The maximal volume measured at a pressure of 40 cm H_2O was recorded as a measure of lung compliance. To collect BALF, the left lung was lavaged three times with 0.9 % NaCl (sal). The BALF samples were pooled and centrifuged at 500 rpm for 5 min. Differential cell counts were obtained on cytospin preparations after a Pappenheim staining (May–Grünwald, Giemsa (20)). Tissue from the right lower lobe was snap-frozen for mRNA analyses. The bronchus to the right upper lobe was cannulated for airway fixation with 10% formalin for 24 h at 30 cm H_2O pressure, followed by transfer into phosphate buffered saline.

RNA Extraction and Reverse Transcription

Snap-frozen lung tissue from the right lower lobe was cut in 30-mg pieces. The tissue was transferred into lysis buffer (RLT buffer Qiagen, Hilden, Germany) for RNA extraction. After vortexing, the suspension was transferred to an RNeasy mini column (Qiagen) and processed according to the manufacturer's protocol. The purity and yield

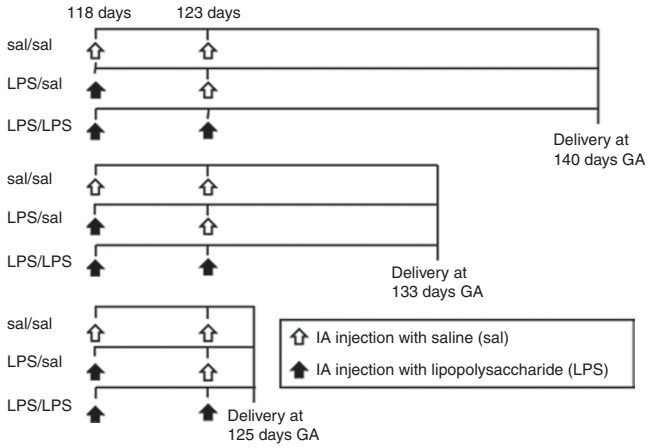

Figure 6. Animal model of intra-amniotic LPS exposure. All animals were exposed to saline (sal) or LPS at 118 and 123 d GA, resulting in three treatment groups: sal/sal (control), LPS/sal, and LPS/LPS. Animals were delivered at three different GAs: 125, 133, and 140 d. GA, gestational age; IA, intra-amniotic; LPS, lipopolysaccharide.

of the RNA were photometrically determined using a Nanodrop spectrophotometer (Thermo Scientific, Wilmington, DE), and 1 µg total RNA was reverse transcribed by addition of 2 µl oligo(dT) primers (10 µmol/l), 1 µl RNase inhibitor (10 units/µl), 2 µl deoxynucleotide Mix (5 mmol/l), and Omniscript transcriptase (0.2 U/µl; Qiagen) and incubation for 1 h at 37 °C. The cDNA was denatured at 93 °C for 5 min.

Real-Time PCR

The design of real-time PCR primers was based on published cDNA sequences (24,38). All PCRs were performed using 1 µg/µl cDNA per reaction in duplicates. Real-time PCR reactions were performed with the LightCycler 480 SYBR Green I Master mix (4707516001, Roche-Applied, Mannheim, Germany) on a LightCycler 480 Instrument according to the manufacturer's instructions. Real-time PCR results of *TLR1*, *TLR2*, *TLR4*, and *TLR6* were normalized to the housekeeping gene ovine ribosomal protein S15 (*ovRPS15*), and mean fold changes in mRNA expression were calculated by the $\Delta\Delta C_t$ method (39).

Immunohistochemistry (PU.1 and Clara Cell Secretory Protein)

Paraffin-embedded lung sections were deparaffinized in an ethanol series, and endogenous peroxidase activity was blocked by incubation with 3% H_2O_2 in milli-Q water. Sections were incubated overnight at 4 °C with the diluted primary antibody. Staining for hematopoietic transcription factor PU.1 (Santa Cruz Biotechnology, Santa Cruz, CA) was performed as described (14,16). After incubation with the appropriate secondary antibody, immunostaining was enhanced with the Vectastain ABC peroxidase Elite kit (Vector Laboratories, Burlingame, CA) and stained with nickel-diaminobenzidine. After counterstaining with Mayer's hematoxylin, the sections were washed and dehydrated. Sections were scored for PU.1 staining with a semiquantitative scoring system: 1, little staining; 2, some staining; and 3, heavy staining. The analysis was performed in a blinded fashion.

A lung-specific Clara cell secretory protein (40) was detected in lung sections that were incubated overnight at 4 °C with the diluted primary antibody (rabbit anti-uteroglobin, Abcam, Cambridge, UK). After incubation with the appropriate secondary antibody, immunostaining was enhanced as described above, stained with diaminobenzidine, and counterstained with Mayer's hematoxylin.

Mast Cell Staining

Mast cell staining was performed on paraffin-embedded lung sections (4 µm, transverse) from the right upper lobe (41). Briefly, the sections were stained with Weigert's iron hematoxylin working solution for 10 min. After rinsing with water, the sections were stained with 1% toluidine blue in 35% ethanol for 1 min. Subsequently, the sections were quickly dehydrated in ethanol and xylol. Microscopic images were taken at ×100 and ×200 magnifications using a Leica microscope and Leica Qwin Pro, version 3.4.0, software (Leica Microsystems, Mannheim, Germany). The circumference of all bronchi was measured at ×100 magnification using ImageJ software, version 1.45 (National Institutes of Health, Bethesda, MD). Mast cells were counted at ×200 magnification in six representative sections per animal. The analysis was performed in a blinded fashion.

Elastin Staining

Sections of lung were incubated for 20 min in Weigert's resorcin–fuchsin (Chroma GmbH, Münster, Germany) at 60–70 °C (41,42). After rinsing with water, the sections were incubated for 3 min in a tartrazine solution at room temperature. Subsequently, the sections were washed and dehydrated in ethanol and xylol. Microscopic images were taken at ×200 magnification, and elastin foci were counted in six representative sections per animal. The analysis was performed in a blinded fashion.

Data Analysis

Results are given as mean ± SE. Comparisons between groups were performed by two-way analysis of variance with Bonferroni *post hoc* analysis (GraphPad Prism, version 5, San Jose, CA). Significance was accepted at $P < 0.05$.

ACKNOWLEDGMENTS

We thank Richard Dalton, Andrea Lee, Carryn McLean, Masatoshi Saito, Clare Berry, Jennifer Henderson, Tim Wolfs, Nico Kloosterboer, and Lilian Kessels for excellent technical support.

STATEMENT OF FINANCIAL SUPPORT

This work was supported by National Institute of Child Health and Human Development Grant HD-57869 (S.G.K.).

Disclosure: The authors declare no conflict of interest.

REFERENCES

1. Goldenberg RL, Hauth JC, Andrews WW. Intrauterine infection and preterm delivery. N Engl J Med 2000;342:1500–7.
2. Gotsch F, Romero R, Kusanovic JP, et al. The fetal inflammatory response syndrome. Clin Obstet Gynecol 2007;50:652–83.
3. Gantert M, Been JV, Gavilanes AW, Garnier Y, Zimmermann LJ, Kramer BW. Chorioamnionitis: a multiorgan disease of the fetus? J Perinatol 2010;30 Suppl:S21–30.
4. Moss TJ, Nitsos I, Kramer BW, Ikegami M, Newnham JP, Jobe AH. Intra-amniotic endotoxin induces lung maturation by direct effects on the developing respiratory tract in preterm sheep. Am J Obstet Gynecol 2002;187:1059–65.
5. Watterberg KL, Demers LM, Scott SM, Murphy S. Chorioamnionitis and early lung inflammation in infants in whom bronchopulmonary dysplasia develops. Pediatrics 1996;97:210–5.
6. Willet KE, Kramer BW, Kallapur SG, et al. Intra-amniotic injection of IL-1 induces inflammation and maturation in fetal sheep lung. Am J Physiol Lung Cell Mol Physiol 2002;282:L411–20.
7. Been JV, Zimmermann LJ. Histological chorioamnionitis and respiratory outcome in preterm infants. Arch Dis Child Fetal Neonatal Ed 2009;94:F218–25.
8. Hartling L, Liang Y, Lacaze-Masmonteil T. Chorioamnionitis as a risk factor for bronchopulmonary dysplasia: a systematic review and meta-analysis. Arch Dis Child Fetal Neonatal Ed 2012;97:F8–F17.
9. Speer CP. Chorioamnionitis, postnatal factors and proinflammatory response in the pathogenetic sequence of bronchopulmonary dysplasia. Neonatology 2009;95:353–61.
10. Jobe AH, Bancalari E. Bronchopulmonary dysplasia. Am J Respir Crit Care Med 2001;163:1723–9.
11. Wolfs TG, Jellema RK, Turrisi G, Becucci E, Buonocore G, Kramer BW. Inflammation-induced immune suppression of the fetus: a potential link between chorioamnionitis and postnatal early onset sepsis. J Matern Fetal Neonatal Med 2012;25 Suppl 1:8–11.
12. Lee AJ, Lambermont VA, Pillow JJ, et al. Fetal responses to lipopolysaccharide-induced chorioamnionitis alter immune and airway responses in 7-week-old sheep. Am J Obstet Gynecol 2011;204:364.e17–24.

13. Kallapur SG, Jobe AH, Ball MK, et al. Pulmonary and systemic endotoxin tolerance in preterm fetal sheep exposed to chorioamnionitis. J Immunol 2007;179:8491–9.
14. Kramer BW, Joshi SN, Moss TJ, et al. Endotoxin-induced maturation of monocytes in preterm fetal sheep lung. Am J Physiol Lung Cell Mol Physiol 2007;293:L345–53.
15. Kramer BW, Kallapur SG, Moss TJ, Nitsos I, Newnham JP, Jobe AH. Intra-amniotic LPS modulation of TLR signaling in lung and blood monocytes of fetal sheep. Innate Immun 2009;15:101–7.
16. Kramer BW, Ikegami M, Moss TJ, Nitsos I, Newnham JP, Jobe AH. Endotoxin-induced chorioamnionitis modulates innate immunity of monocytes in preterm sheep. Am J Respir Crit Care Med 2005;171:73–7.
17. Czikk MJ, McCarthy FP, Murphy KE. Chorioamnionitis: from pathogenesis to treatment. Clin Microbiol Infect 2011;17:1304–11.
18. Kallapur SG, Nitsos I, Moss TJ, et al. Chronic endotoxin exposure does not cause sustained structural abnormalities in the fetal sheep lungs. Am J Physiol Lung Cell Mol Physiol 2005;288:L966–74.
19. Newnham JP, Kallapur SG, Kramer BW, et al. Betamethasone effects on chorioamnionitis induced by intra-amniotic endotoxin in sheep. Am J Obstet Gynecol 2003;189:1458–66.
20. Kramer BW, Moss TJ, Willet KE, et al. Dose and time response after intraamniotic endotoxin in preterm lambs. Am J Respir Crit Care Med 2001;164:982–8.
21. Kallapur SG, Willet KE, Jobe AH, Ikegami M, Bachurski CJ. Intra-amniotic endotoxin: chorioamnionitis precedes lung maturation in preterm lambs. Am J Physiol Lung Cell Mol Physiol 2001;280:L527–36.
22. Shibata Y, Berclaz PY, Chroneos ZC, Yoshida M, Whitsett JA, Trapnell BC. GM-CSF regulates alveolar macrophage differentiation and innate immunity in the lung through PU.1. Immunity 2001;15:557–67.
23. Berclaz PY, Carey B, Fillipi MD, et al. GM-CSF regulates a PU.1-dependent transcriptional program determining the pulmonary response to LPS. Am J Respir Cell Mol Biol 2007;36:114–21.
24. Hillman NH, Moss TJ, Nitsos I, et al. Toll-like receptors and agonist responses in the developing fetal sheep lung. Pediatr Res 2008;63:388–93.
25. Shen CM, Lin SC, Niu DM, Kou YR. Development of monocyte Toll-like receptor 2 and Toll-like receptor 4 in preterm newborns during the first few months of life. Pediatr Res 2013;73:685–91.
26. Brown JM, Wilson TM, Metcalfe DD. The mast cell and allergic diseases: role in pathogenesis and implications for therapy. Clin Exp Allergy 2008;38:4–18.
27. Kumar R, Yu Y, Story RE, et al. Prematurity, chorioamnionitis, and the development of recurrent wheezing: a prospective birth cohort study. J Allergy Clin Immunol 2008;121:878–84.e6.
28. Getahun D, Strickland D, Zeiger RS, et al. Effect of chorioamnionitis on early childhood asthma. Arch Pediatr Adolesc Med 2010;164:187–92.
29. Prussin C, Metcalfe DD. 4. IgE, mast cells, basophils, and eosinophils. J Allergy Clin Immunol 2003;111(2 Suppl):S486–94.
30. Bhattacharya S, Go D, Krenitsky DL, et al. Genome-wide transcriptional profiling reveals connective tissue mast cell accumulation in bronchopulmonary dysplasia. Am J Respir Crit Care Med 2012;186:349–58.
31. Pillow JJ, Jobe AH, Collins RA, et al. Variability in preterm lamb lung mechanics after intra-amniotic endotoxin is associated with changes in surfactant pool size and morphometry. Am J Physiol Lung Cell Mol Physiol 2004;287:L992–8.
32. Cao L, Wang J, Tseu I, Luo D, Post M. Maternal exposure to endotoxin delays alveolarization during postnatal rat lung development. Am J Physiol Lung Cell Mol Physiol 2009;296:L726–37.
33. Moss TJ, Newnham JP, Willett KE, Kramer BW, Jobe AH, Ikegami M. Early gestational intra-amniotic endotoxin: lung function, surfactant, and morphometry. Am J Respir Crit Care Med 2002;165:805–11.
34. Kuypers E, Collins JJ, Kramer BW, et al. Intra-amniotic LPS and antenatal betamethasone: inflammation and maturation in preterm lamb lungs. Am J Physiol Lung Cell Mol Physiol 2012;302:L380–9.
35. Wolfs TG, Buurman WA, Zoer B, et al. Endotoxin induced chorioamnionitis prevents intestinal development during gestation in fetal sheep. PLoS ONE 2009;4:e5837.
36. Kemp MW, Kannan PS, Saito M, et al. Selective exposure of the fetal lung and skin/amnion (but not gastro-intestinal tract) to LPS elicits acute systemic inflammation in fetal sheep. PLoS ONE 2013;8:e63355.
37. Jobe AH, Kramer BW, Moss TJ, Newnham JP, Ikegami M. Decreased indicators of lung injury with continuous positive expiratory pressure in preterm lambs. Pediatr Res 2002;52:387–92.
38. Seehase M, Gantert M, Ladenburger A, et al. Myocardial response in preterm fetal sheep exposed to systemic endotoxinaemia. Pediatr Res 2011;70:242–6.
39. Livak KJ, Schmittgen TD. Analysis of relative gene expression data using real-time quantitative PCR and the 2(-Delta Delta C(T)) Method. Methods 2001;25:402–8.
40. Singh G, Katyal SL. Clara cells and Clara cell 10 kD protein (CC10). Am J Respir Cell Mol Biol 1997;17:141–3.
41. Kramer BW, Albertine KH, Moss TJ, et al. All-trans retinoic acid and intra-amniotic endotoxin-mediated effects on fetal sheep lung. Anat Rec (Hoboken) 2008;291:1271–7.
42. Collins JJ, Kallapur SG, Knox CL, et al. Inflammation in fetal sheep from intra-amniotic injection of Ureaplasma parvum. Am J Physiol Lung Cell Mol Physiol 2010;299:L852–60.